Discrimination between Small Earthquakes and Local Quarry Blasts Using Committee Machine

Ahmed Lethy (alethy@nriag.sci.eg)
National Research Institute of Astronomy and Geophysics
Adel Othman
National Research Institute of Astronomy and Geophysics
Mohamed ElGabry
National Research Institute of Astronomy and Geophysics
Hesham Hussein
National Research Institute of Astronomy and Geophysics
Gad El-Qady
National Research Institute of Astronomy and Geophysics

Research Article

Keywords: Earthquakes, Artificial neural network, Committee Machine, k-means, Self-Organized Map

Posted Date: June 7th, 2021

DOI: https://doi.org/10.21203/rs.3.rs-588073/v1

Discrimination between Small Earthquakes and Local Quarry Blasts Using Committee Machine

Ahmed Lethy*, Adel S. Othman, Mohamed N. ElGabry, Hesham Hussein, Gad El-Qady

National Research Institute of Astronomy and Geophysics NRIAG, 11421 Helwan Egypt

***Corresponding author**

Ahmed lethy

Email:**ahmedellethy@gmail.com**

https://orcid.org/0000-0002-9533-4905

permanent address

National Research Institute of Astronomy and Geophysics NRIAG, 1, El Marsad St. 11421, Helwan Egypt.

Authorship Statement

Ahmed Lethy performed the data analysis and wrote the manuscript; Adel S. Othman preparation of the data set; Mohamed N. ElGabry contributed to the conception of the study and revise the manuscript; Hesham Hussein revise the manuscript with constructive discussion; Gad El-Qady revise the manuscript.

Abstract

A combination of multiple discrimination artificial neural networks using different seismic source parameters is suggested using a committee machine. In this work, a committee machine was used to combine supervised and unsupervised artificial neural networks to discriminate between earthquakes and quarry blasts using data from the Egyptian National Seismological Network (ENSN). The unsupervised network is used as a measure of accuracy for the results of the supervised neural network. The unsupervised Self-Organized Map (SOM) and the k-means clustering algorithms are used to estimate support and confidence measures for the results. Meanwhile, the supervised neural network is used to discriminate between earthquakes and explosions.

The artificial neural networks are trained using different input parameters which are the P wave spectrum corner frequency (P_{cF}), S wave corner frequency (S_{cF}), and the ratio (R_{cf}) of P_{cF} to S_{cf}. The combined approach succeeds to discriminate between earthquakes and quarry blasts in Northern Egypt. The method provides the results with a measure of confidence which eliminates false discrimination.

The current paper represents an idea to implement artificial intelligence to assist experts in decision-making situations. The committee machine could identify the nature of a particular event, using the aid of several discrimination methods. The proposed committee machine could combine the results of several algorithms and expert opinions to form one single output with a confidence measure.

Keywords

Earthquakes, Artificial neural network, Committee Machine, k-means, Self-Organized Map

Introduction

Both explosions and earthquakes release a large amount of acoustic energy that ripples through the earth and recorded by seismic stations; thanks to the difference in source dynamics, the recorded waveform may look different. But it is still a job that needs trained analysts to conduct such discrimination, which is very critical to clean seismic catalogs from possible explosions and provide monitoring tools for controlling such blasts in vast areas for security and proliferation.

Different discriminating methods have been previously proposed based on waveform amplitude ratios [1–4], or spectral methods[5–13], or even coda based methods [14,15]. Also, discrimination was proposed based on the time of the day seismicity maps where quarries blasts are usually carried out during the early hours of the day[16,17]. In addition, pattern recognition techniques have been used for seismic discrimination [18,19]

Nevertheless, many attempts have been made to discriminate between earthquakes and man-made seismic sources using neural network[6,9,20–25]. Tiira[26] used a multilayer perceptron (MPL) to discriminate between nuclear explosions and earthquakes. Del Pezzo et al.,[27] used a neural network to discriminate between earthquakes and underwater chemical explosions fired by fishermen in Pozzuoli bay.

Nowadays, with the expansion in the use of explosive demolition-based techniques in mining and new infrastructure projects, it became very crucial to distinguish between naturally occurring from man-made seismic events. Identification of the event's nature is urgently required for decision-makers. Without true verification from the ground, experts use different published methods for discrimination. However, these methods have different results, rising argue about confidence and depend mainly on the analyst experience. Therefore, we develop an automated expert artificial neural network that could combine the results of different methods and produce a single output with a confidence measure. This expert artificial neural network is a committee machine with the ability to identify the nature of a particular event, using the aid of several discrimination methods. The proposed committee machine could combine the results of several algorithms and expert opinions to form one single output with a confidence measure. The confidence measure is estimated using unsupervised Self-Organized Map (SOM) and the k-means clustering algorithms.

Data Set

The data set used in this study are seismic events (natural earthquakes and explosions) recorded by the Egyptian National Seismological Network (ENSN)[28–30]. This data set was recorded within the Northern part of Egypt (Figure 1). The events were selected during the period from 2009 to 2015. These events have a duration magnitude ranging from 1.5 to 3.3, epicentral distances up to 200 km, and depth shallower than 25 km. The earthquakes and explosions events have a comparable magnitude range. Figure 2, shows the duration magnitude histograms for both earthquakes and explosions. The histograms show similar occurrence frequency distribution for both earthquakes and explosions.

The dataset contains 720 events where 354 of these events are earthquakes and 366 events represent local quarry explosions. The data set is formed of two main seismic source parameters that are hypocenter parameters and spectral parameters. The hypocenter parameters (origin time, epicentral distance, latitude, longitude, focal depth, and duration magnitude) are collected from the ENSN bulletins. Meanwhile, the seismic source spectral parameters are estimated using the EQK_SRC_PARA software[31]. The used parameters are the duration magnitude (Md), P-wave spectrum corner frequency (P_{cf}), S-wave corner frequency (S_{cf}), and the ratio (R_{cf}) of P_{cf} to S_{cf}.

The parameters dependency could be investigated through the correlation matrix listed in Table 1. The corner frequencies of the P and S waves spectrum are highly correlated (the correlation coefficient is 0.96). Meanwhile, the corner frequencies and their ratio are uncorrelated with the duration magnitude, indicating that the corner frequencies are independent of the duration magnitude.

The events distribution over the four parameters is represented in (Figure 3). The scatter plot (Figure 3), shows a continuous distribution of events along the range of each parameter. Remarkably, the corner frequencies and their ratio are almost separating the earthquakes from the explosion events with a small overlap. This may be attributed to the time delays of the ripple-fired quarry blasts in the northern part of Egypt[32]. These ripple-fired explosions have a characteristic spectrum due to the time delay between detonations[6,33–38].

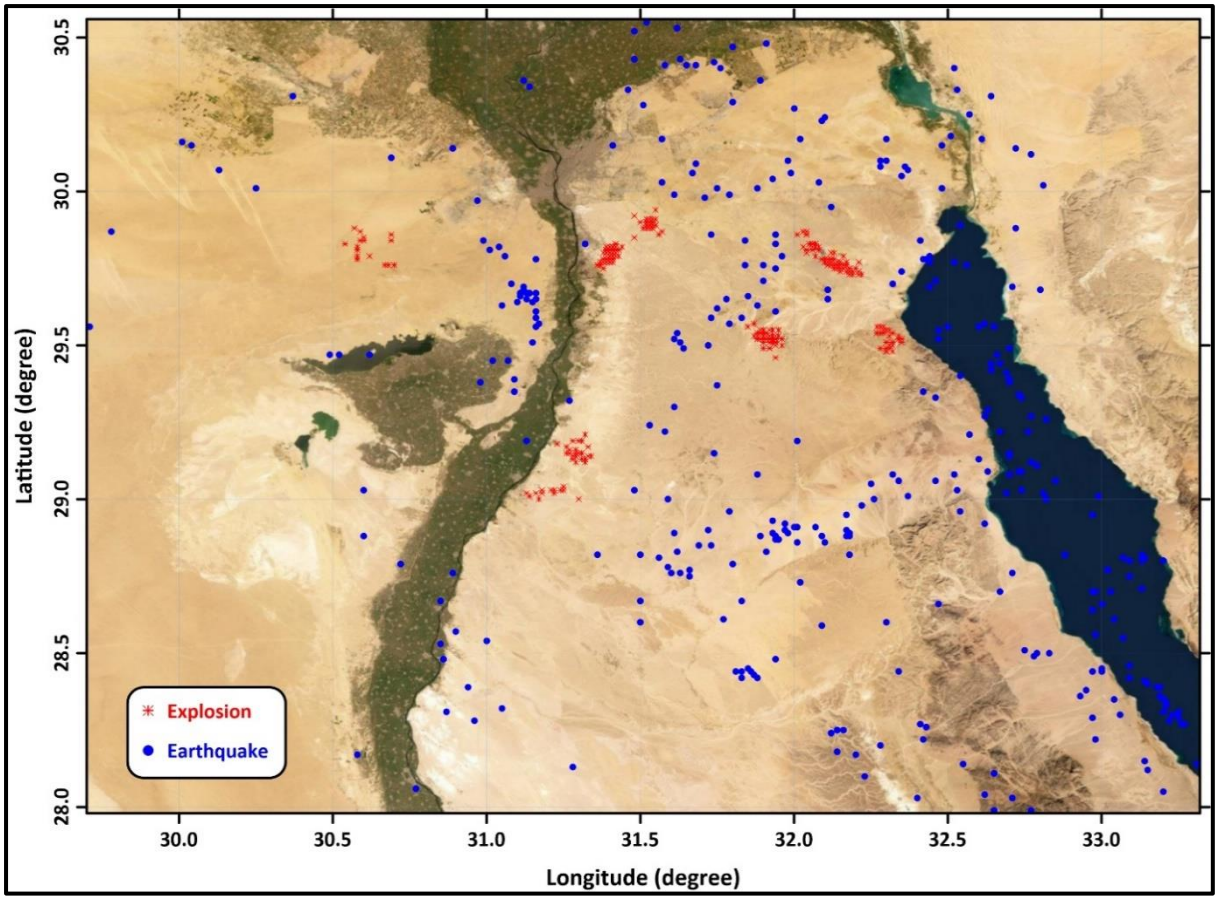

Figure 1:Events spatial distribution.

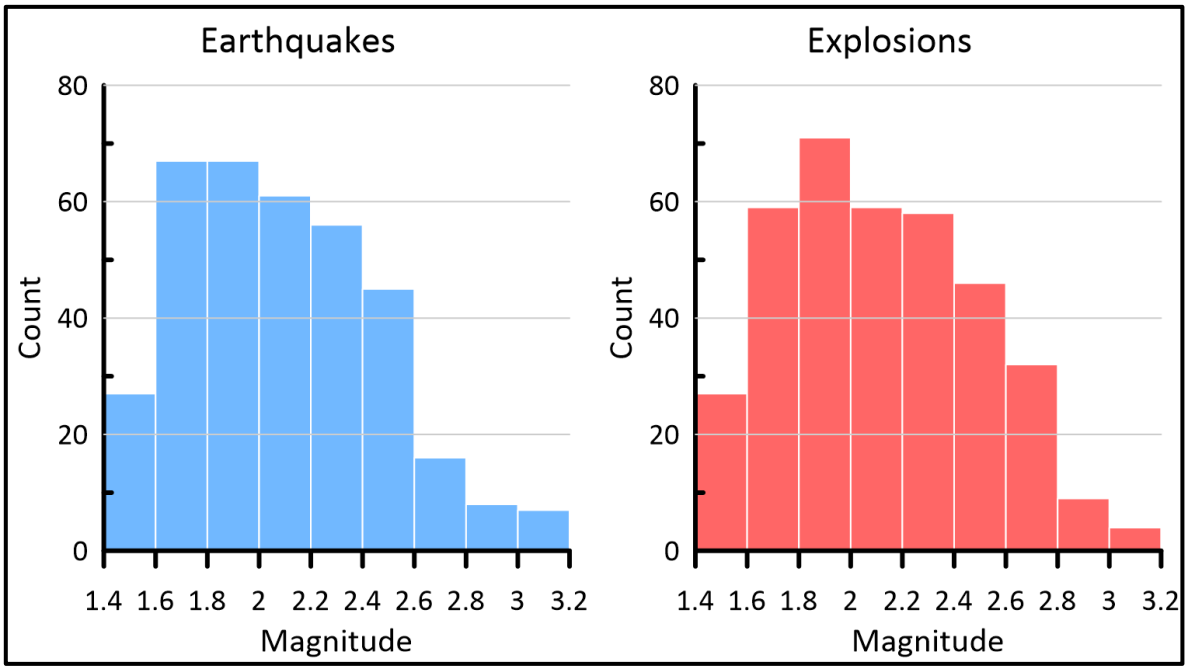

Figure 2: The occurrence frequency of duration magnitude of earthquakes (left) and explosions (Right).

Table 1: The correlation coefficients between the four parameters

	Md	P_{cf}	S_{cf}	R_{cf}
Md	1	-0.37	-0.28	0.029
P_{cf}		1	0.96	-0.65
S_{cf}			1	-0.81
R_{cf}				1

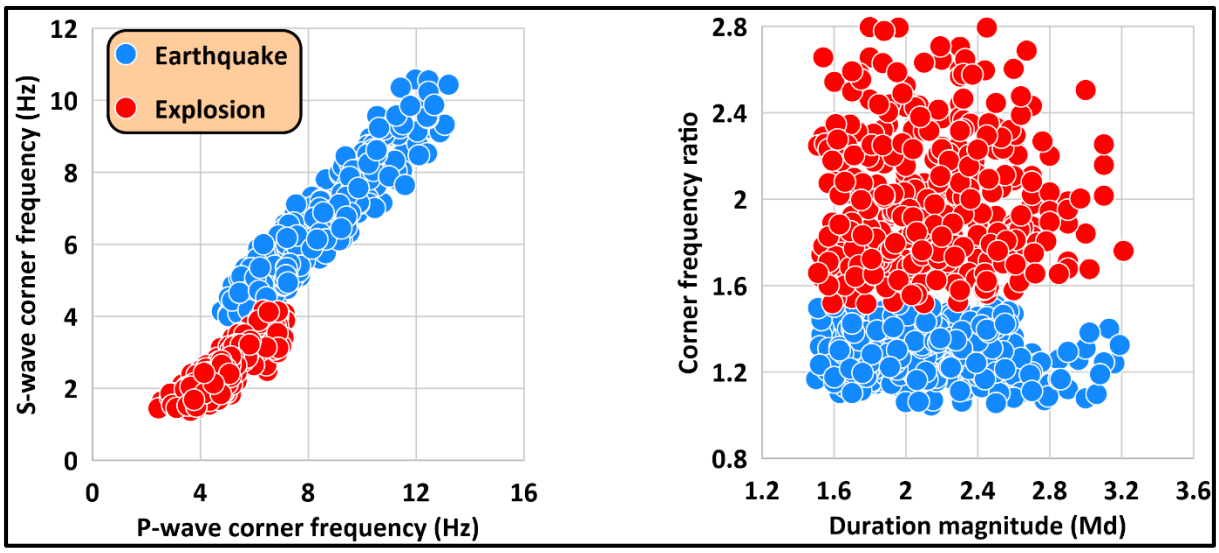

Figure 3: P-wave cornel frequency versus S-wave cornel frequency and the duration magnitude versus corner frequency ratio. The blue dots represent earthquakes and the red dots represent explosions.

Method

Artificial Neural Network (ANN)

The artificial neural network (ANN) became very popular in the last decade. It is a computational scheme that tries to simulate the neuronal biological systems. The artificial neural network consists of various interconnected units (neurons/nodes).Artificial neural network has been widely used for detecting seismic events[39] and even for velocity model inversion[40].

A common neural network structure formed of three layers, called input, hidden, and output layers were used in this study[41,42]. Each layer consists of one or more neurons where the values from the input layer, Xi, is sent to all neurons in the hidden layer in a fully interconnected structure. The values entering neurons in the hidden layer, Nj, are multiplied by weights, Wij. Then the weighted inputs are summed together and feed to a mathematical function (known as activation function) that bounds the neuron output. The data flow is in one direction from the input layer passing through the hidden layer towards the output layer. This type of neural network is known as a feedforward network[43].

The neural networks were trained using the Levenberg-Marquardt algorithm[44–46] in a batch training mode. Where, all the training samples are passed to the network in advance to update the network weights [46,47]. The objective of the training function is to minimize the batch error between the calculated and actual values using mean square error (MSE).

The learning data set was divided randomly into three sets containing 70%, 15%, and 15% of the data. The training set, that 70 % of the data were used to train the neural to achieve the required targets. The validation set contains 15% of the data to validate the training progress throughout the training process. Finally, the test set contains 15% of the data used to test the neural after training. Four pairs of ANNs were developed to discriminate between earthquakes and explosions using different input data sets. The first three pairs of ANNs have a single parameter (either the $\{P_{cf}\}$, $\{S_{cf}\}$ or $\{R_{cf}\}$) in the input set while the last pair of ANNs has the three parameters in the input set $\{P_{cf}, S_{cf}, R_{cf}\}$.

In a supervised training, the neural is trained to output a specific target set. The pairs of ANNs were trained with two distinct target sets. The first target set is the source depth, where the explosions have zero depth and the earthquakes have deeper depths. Meanwhile, the second target set was a binary set formed of ones for earthquakes and zeros for explosions. The networks were trained to produce 1 for earthquakes and 0 for explosions. So, eventually we end up with eight ANNs.

Each neural network was trained several times (epochs) to reach the specified target set. During each epoch, the network goes through all the training samples and then updates its coefficients based on the MSE. Then the data of the validation and test sets are applied to the neural network and the MSE errors are computed. To be sure that the neural network is not memorizing the training set, the neural network coefficient set that produces the best validation results is used for discrimination.

Usually, the overall performance of the ANN is measured using mean square error (MSE), mean absolute error (MAE), and the correlation coefficient (R) between the estimated (y) and the actual (x) values as follows:

$$MSE = \frac{\sum_{i=0}^{n}(y_i - x_i)^2}{n}, \quad (1)$$

$$MAE = \frac{1}{n}\sum_{i=0}^{n}|y_i - x_i|, \quad (2)$$

$$R = \frac{n\sum_{i=0}^{n} x_i y_i - \sum_{i=0}^{n} x_i \sum_{i=0}^{n} y_i}{\sqrt{n\sum_{i=0}^{n} x_i^2 - \left(\sum_{i=0}^{n} x_i\right)^2}\sqrt{n\sum_{i=0}^{n} y_i^2 - \left(\sum_{i=0}^{n} y_i\right)^2}}, \quad (3)$$

By considering the ANN as a function of the input and target sets, then eight ANNs could be defined in the form ANN (input set, target set). The performance results of the eight ANNs are listed in Table 2. The MSE and MAE could be misleading in the comparison between the ANNs that have the depth as a target set and those that have the binary target set as both sets have different ranges and different units (the depth is km and the binary is unitless). Therefore, the correlation coefficient R is more suitable for such a comparison.

For the same input set, the performance is enhanced for the binary target set. The best performance was for the ANN with the ratio of the cornel frequencies R_{cf} as input parameter and the binary target set $ANN(\{R_{cf}\}, binary)$. This indicates that the R_{cf} has a more separation capability than the other parameters (also this could be deduced from Figure 3). In the training phase, the $ANN(\{R_{cf}\}, binary)$ and $ANN(\{P_{cf}, S_{cf}, R_{cf}\}, binary)$ has the highest performance. Meanwhile in the validation phase, the $ANN(\{R_{cf}\}, binary)$ has the highest performance and $ANN(\{P_{cf}, S_{cf}, R_{cf}\}, binary)$ has a slightly lower performance. Finally, the $ANN(\{P_{cf}, S_{cf}, R_{cf}\}, binary)$ has the highest performance in the test phase.

Eventually, the overall performance of the ANN is computed over the unity of the three sets (training, validation, and test) while the most important part is the test set where it indicates the ability of the ANN for generalization[48]. The test set is relatively small in comparison to the input sample space. A larger test set could produce a relatively larger error.

Table 2: The performance of the ANNs

ANN		Training		Validation		Test		All		
Input parameter	**Target set**	**MSE**	**R**	**MSE**	**R**	**MSE**	**R**	**MSE**	**R**	**MAE**
P_{cf}	Depth	31.562	0.678	30.955	0.714	29.413	0.702	31.148	0.687	3.877
P_{cf}	0/1	0.080	0.825	0.089	0.803	0.080	0.825	0.081	0.822	0.183
S_{cf}	Depth	20.697	0.808	15.725	0.845	21.253	0.804	20.035	0.813	2.670
S_{cf}	0/1	0.005	0.990	0.010	0.979	0.017	0.966	0.008	0.985	0.015
R_{cf}	Depth	19.365	0.815	21.628	0.851	18.254	0.804	19.538	0.818	2.609
R_{cf}	0/1	0.002	**0.996**	0.000	**1.000**	0.004	0.992	0.002	**0.996**	0.010
P_{cf} ,S_{cf} , R_{cf}	Depth	22.391	0.794	15.296	0.850	11.946	0.888	19.760	0.816	2.973
P_{cf} ,S_{cf} , R_{cf}	0/1	0.002	**0.996**	0.004	0.993	0.003	**0.994**	0.003	0.995	0.025

Generally, the performance is very high indicating that the ANNs are well trained (at least for the last 5 ANNs in Table 2). Unfortunately, well trained ANN could occasionally produce unreliable results. The results of the eight ANNs are presented in Figure 4. This figure represents the fitting between the estimated and the actual target sets. Perfect results should be aligned along a 45-degrees line. Histograms in the plots indicated the amplitude and frequency of the errors. This figure shows that even with high-performance neural networks several events were misclassified (e.g., Figure 4 (f) the correlation coefficient is relatively high R=0.985 and the error measures are very low MSE=0.008 & MAE=0.015, even so, several events were misclassified).

To enhance the results, the output of each pair of the ANNs that has the same input parameter are combined. The combination is done through a simple mathematical condition. The ANN could be considered as a function of the target set and the combined ANN (ANNC) could be defined as:

$$\text{ANNC} = \begin{cases} 1 \; if \; ANN(depth) > 2 \; and \; ANN(binary) > 0.5 \\ 0 \; otherwise \end{cases}, \quad (4)$$

Therefore, any event is declared as an Earthquake, if the output of the ANN that has the source depth as the target set is greater than 2 and the output of the ANN that has the binary set as target set is greater than 0.5. Otherwise, the event is declared to be an explosion.

This simple combination enhances the result significantly. Figure 5 shows the combined results of the ANNs. The outputs of each successive pair of the eight ANNs listed in Table 2 are combined to produce four ANNCs labeled ANN1 to ANN4 as depicted in Figure 5. The first combined ANNs has 83 mistakes and the second has only 6 mistakes. While the third and fourth combined ANNs (Figure 5 c & d) almost have 100 percentage accurate discrimination (720 and 719 correct discriminations respectively). However, this may not be true for any other events that were not part of the learning data set. Therefore, ±0.05 percent of random noise was added to the learning data set. This random error could account for miss picking of the cornel frequencies in the real situation. The results are shown in Figure 6. The ANNs are still capable of discriminating with few mistakes. The total mistakes are 123, 8, 13,

and 3 for the ANN1, ANN2, ANN3, and ANN4 respectively. This indicates that for future event discrimination any ANN of the listed ANNs could produce a wrong classification. Therefore, the discrimination process can't depend on any of them alone.

Moreover, the ANN has no measure of accuracy for any new input that was not part of the learning data set. To deduce such a measure, the Self-organized Map (SOM) clustering and K-means clustering techniques were combined to produce what is known as support and confidence measures [49,50]. These techniques will be explained in the coming sections.

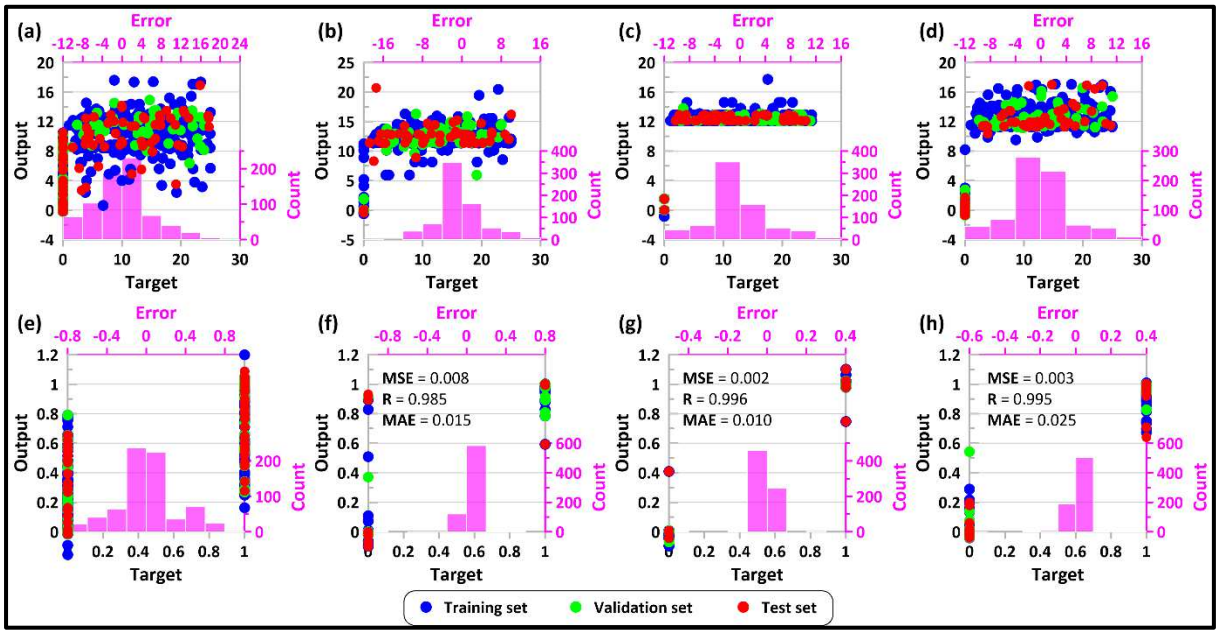

Figure 4: The results of the eight ANNs. The above row represents ANNs with the depth as the target set while the lower row represents ANNs with 0/1 as the target set. Error histograms are present in each panel. (a & e) The ANNs input parameter is P_{cf}. (b & f) The ANNs input parameter is S_{cf}. (c & g) The ANNs input parameter is R_{cf}. (d & h) The ANNs input parameters are P_{cf}, S_{cf}, R_{cf}.

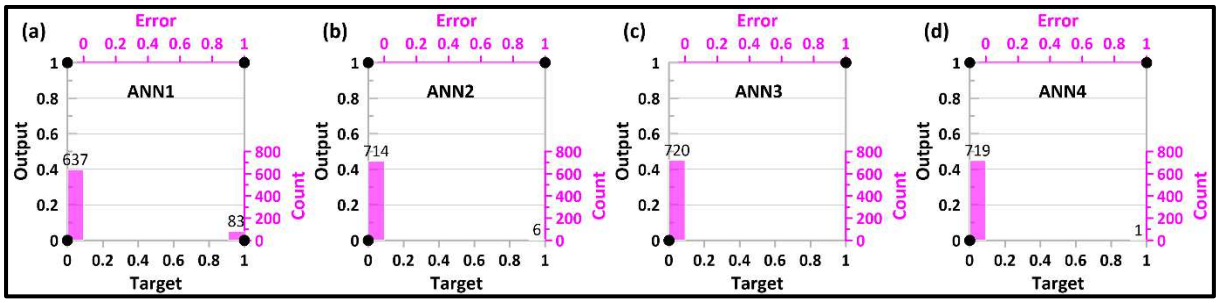

Figure 5: The combined results of the ANNs. The histograms present the absolute values of the errors.

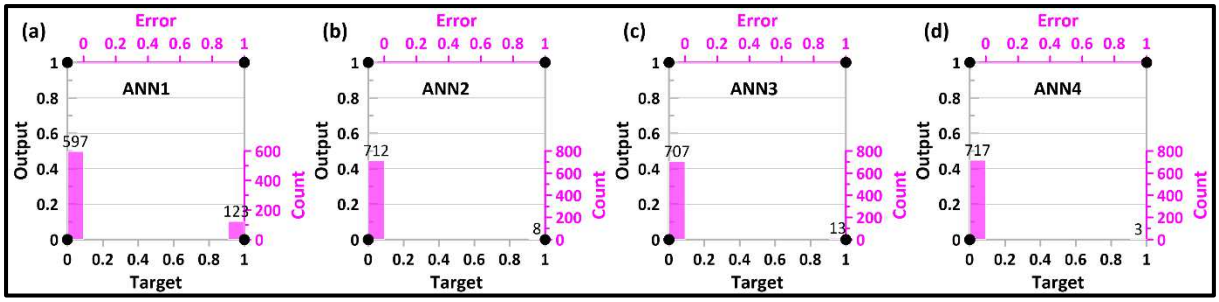

Figure 6: The results of the combined ANNs with ±0.05% random noise embedded in the input data. The histograms show the absolute values of the errors.

Self-organizing map clustering (SOM)

The Self-organizing map (SOM) is a type of neural network that can perform clustering using competitive learning which is an unsupervised learning technique. Du[51] gave a good review of neural network clustering. Flexer[52] discussed the application of SOM for clustering and data visualization. Roden et al.,[53] implemented SOM to analyze several seismic attributes to identify natural patterns for stratigraphic interpretation. Meanwhile, Köhler et al.[54] used SOMs to detect and classify events in continuous seismic wavefield records also the SOM was able to visualize the 24-hour human activity cycle. Kuyuk et al.,[55] applied SOM for discriminating between earthquakes and quarry blasts using the complexity, spectral ratio, S/P wave amplitude peak ratio, and origin time of events as the input parameters. Messina & Langer[56] used the SOM to classify volcanic tremor.

The neurons in the SOM are arranged in a two-dimensional array/lattice. Each neuron is a vector with the dimensionality of the input vector. The connections between adjacent neurons define the SOM topology. The SOM can preserve the topology in the projection of the input data from high-dimensional space onto the two-dimensional SOM lattice in a way that relative distances between data points are preserved [57,58]

Different SOM topologies have been investigated by several researchers[57,59,60]. The neurons are commonly connected via square or hexagonal topology. The hexagonal topology is used in this work because it has the highest number of connections between adjacent neuron The SOM is used to classify the dataset into 9 clusters based on the three parameters (P_{cf}, S_{cf}, R_{cf}) and into 4 clusters based on every single parameter. The events were grouped in one of the groups by similarity according to the Euclidean distance between parameters. The results of SOM are usually represented by hits and weights positions plots. Figure 7, shows the topology, connections, and the number of hits per cluster. Remarkably, some clusters are dominated by a single event type. Meanwhile, Figure 8 shows a 3D plot of the distribution of the events over the 9 clusters with the estimated SOM weights positions marked within each parameter. It should be noted that the clusters have overlapping ranges over the three parameters.

Each cluster C contains a number of events "hits" (nE). Some of them represent Earthquakes (nEq) and the others represent explosions (nEx).

The support and confidence measures [49,50] for these clusters could be defined as follows:

The cluster support value (SC)is the ratio of the number of events in that cluster to the total number of events (TE).

$$SC = nE/TE, \quad (5)$$

The confidence of a certain type of event in a given cluster is the ratio of the number of events of that type in the given cluster to the number of events in that cluster.

The confidence of earthquakes of a given cluster is $CfEq = nEq/nE$, (6)

The confidence of explosions of a given cluster is $CfEx = nEx/nE$, (7)

For simplicity, these ratios could be presented as a percentage. The support and confidence measures of the nine clusters are listed in Table 3, while those of the 4 clusters are listed in Table 4.

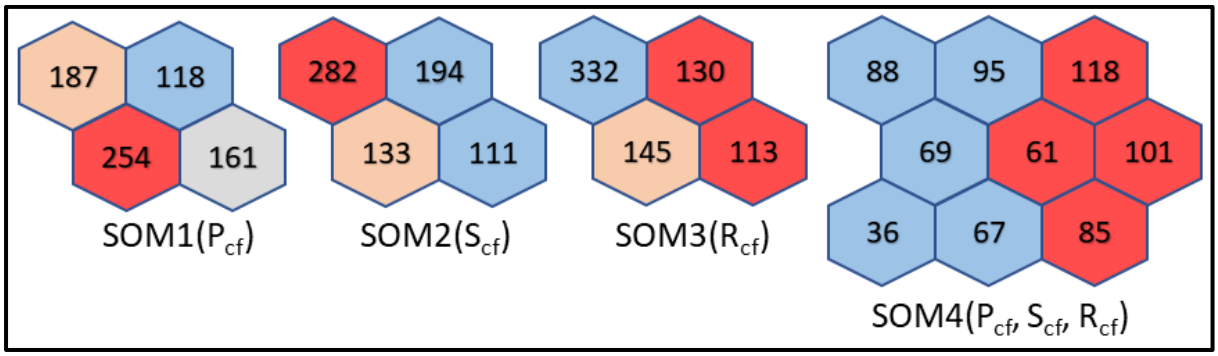

Figure 7: Clusters hits plot. The number of events in each cluster is shown with the cluster color indicating the dominant event-type. Red-colored clusters are dominated by explosions while blue-colored clusters are dominated by earthquakes. The hexagons are representing the neurons and their adjacent sides are representing the connections between neurons.

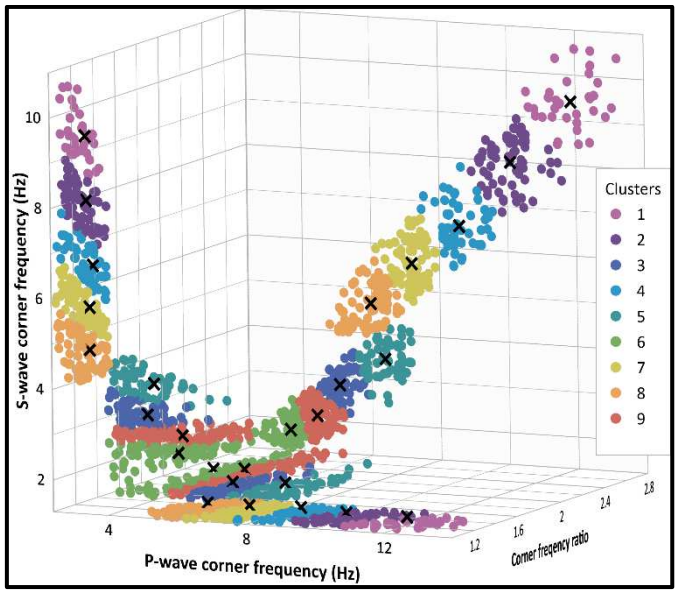

Figure 8:The events distribution over the 9 clusters and the estimated SOM weight positions within each parameter are marked by X.

Table 3: The estimated support and confidence measures of the nine clusters presented as a percentage for clarity.

Cluster	**1**	**2**	**3**	**4**	**5**	**6**	**7**	**8**	**9**
No. of events (nE)	36	67	85	69	61	101	88	95	118
No. of Earthquakes (nEq)	36	67	**0**	69	**0**	**0**	88	94	**0**
No of Explosions (nEx)	**0**	**0**	85	**0**	61	101	**0**	1	118
Support (SC) %	5.0	9.3	11.8	9.5	8.4	14.0	12.2	13.2	16.4
Confidence ($CfEq$) %	100	100	0.0	100	0.0	0.0	100	98.95	0.0
Confidence ($CfEx$) %	0.0	0.0	100	0.0	100	100	0.0	1.05	100

Table 4: The estimated support and confidence measures of the 4 clusters of each parameter.

Parameter	**Cluster**	nE	nEq	nEx	SC (%)	$CfEq$ (%)	$CfEx$ (%)
P_{cf}	1	254	1	253	35.28	0.39	99.61
	2	161	139	22	22.36	86.34	13.66
	3	187	96	91	25.97	51.34	48.66
	4	118	118	**0**	16.39	100	0.0
S_{cf}	1	133	49	84	18.47	36.84	63.16
	2	111	111	**0**	15.42	100	0.0
	3	282	**0**	282	39.17	0.0	100
	4	194	194	**0**	26.94	100	0.00
R_{cf}	1	145	22	123	20.14	15.17	84.83
	2	113	**0**	113	15.69	0.0	100
	3	332	332	**0**	46.11	100	0.0
	4	130	**0**	130	18.06	0.0	100

k-means clustering

The *k*-means algorithm partitions a dataset into subsets by minimizing the mean square error between the center of the cluster and the elements in the same cluster. *k*-means are unsupervised clustering techniques. It requires a predetermined number of clusters. *k*-means clustering algorithms are discussed in detail in [51,61–64]. Kuyuk et al.[65] used the k-means to classify the seismic activities.

The main idea in *k*-means clustering is to find the center of each subset/cluster. The optimum location of the center is obtained as the average of the members in the subset [51]. Using the clusters obtained by the SOMs, the number of clusters is predetermined and the centers could easily be obtained by finding the mean of the members of each cluster using Euclidean distance. Actually, the centers are very close to the SOM weights positions (Figure 8) and almost overlay each other.

Committee machines

The committee machine is utilizing the divide and conquer strategy in which the output of multiple neural networks (experts) are combined to produce a single outcome [41,66,67]. The committee machine has been used in several applications. Mazurov & Polyakova[68], gave a brief history and applications with the mathematical background of the committee theory. Nadiri et al.[69], used a supervised

committee machine for the prediction of fluoride concentration in groundwater. Pandey et al.[70] used a committee machine for the prediction of the currency exchange rate.

The trial-and-error technique is commonly practiced with neural networks to find the best neural network structure that produces the best performance. Therefore, many different neural networks (different structure, number of layers, and the number of neurons per layer) are trained and only the one with the best performance is used. The performance is measured over the training, validation, and test sets which usually do not cover the entire input space. This technique has two drawbacks. First, the network with the best performance on these sets is not necessary to have the best performance over any other sets of the input space. It is not necessary to have the best performance over the three sets. The $ANN(\{R_{cf}\}, binary)$ (Table 2) has the best performance but not over the test set. Second, wasting all the efforts involved in the training of the discarded networks.

The committee machine could overcome these drawbacks. The committee machine can offer better performance than any individual constituent neural network. Although the ANNs have an identical configuration and are trained with similar data, they are trained with different initial conditions. Therefore, they usually converge to different local minima. Committee machines use different combination algorithms to combine the results. The combiner function could be simple as averaging or more complex as a nonlinear gating function [41]. However, in this work, an ANN was used as a combination function for the result of different discrimination methods as well as the results of the trained ANNs.

The committee machine will tend to follow the inputs that are best matching the target, which happens to be of the ANN4. To overcome this issue, intentionally, randomly manipulate the results of the four ANNs (ANN1 to ANN4) to reach 20% wrong classification. So, the input from the four combined ANNs has the same priority during the training process of the committee machine.

Discrimination procedure

The discrimination algorithm consists of three stages.

Stage 1 (ANN)

For any new event of an unknown source, the three parameters are estimated using the EQK_SRC_PARA software [31] as indicated earlier.

This data is feed to the ANNs presented in Figure 4 and listed in Table 2. Then the results are combined using Eq. (4). The output of this stage is four event-type.

Stage 2 (finding the holding cluster)

The inputs of this stage are the event spectral parameters (P_{cf}, S_{cf}, R_{cf}) and the combined networks ANN1 to ANN4 estimated event-type. The event parameters are used to find the SOM holding cluster using the k-means centers. In each SOM of the four SOMs presented in Figure 7, the event will belong to the cluster with the closest k-mean center.

Holding cluster (e)=$\arg \min_{i\in\{1,\dots,m\}} \|e - C_i\|$

Where *m* is the number of clusters, C_i is the k-mean center of cluster number *i*. e=(P_{cf}, S_{cf}, R_{cf}),

Every cluster in the SOM has a support measure and each event-type within that cluster has a confidence value as listed in Tables 3 & 4. The output of this stage is the support and confidence of the holding clusters from the four SOMs for the designated event-type.

Stage 3 (Committee machine)

The inputs of this stage are the combined networks ANN1 to ANN4 estimated event-type with their corresponding SOM support and confidence measures. These data are feed to the committee machine ANN combiner to produce the final output. The output of this stage is the event-type with a confidence measure.

Stage 4 (Measures update)

After verification and approval of the resulted event-type, the number of events in holding clusters is incremented and its support and confidence measures are recomputed.

Discussion and Conclusion

The neural networks were not able to estimate the depth of the earthquake. Also, it produces relatively low or negative depths for explosions.

Even though the neural network fails to estimate the depths of the earthquakes, it separates the earthquake events from the explosion events by produce different depth ranges for both (Figure 4c). The neural were not able to estimate the depths of the earthquakes, because the number of samples representing any single depth value is relatively low.

A simple combination was applied to the results of the ANNs trained with the same parameter, however, they trained to produce different outputs either the depth or binary output (1 for earthquakes and 0 for explosions). This combination is a simple form of committee machine applied in the first stage.

The simple combination applied to the ANN outputs enhances the result significantly. The combined results of the ANN trained with the corner frequency ratio R_{cf} and the ANN trained with the three parameters almost have 100 percentage correct discrimination. These results indicate that the R_{cf} parameter is significantly characterizing the earthquakes from the explosions.

The nine cluster SOM almost separates the earthquakes and explosions in different clusters. All the clusters contain a single event-type except cluster 8 which contains 94 earthquakes and only one explosion. To visualize the result of these SOM clusters the events were posted on a satellite map with the holding cluster number indicated with different shapes (Figure 9). The green-colored asterisks (cluster 5) are almost concentrated in a single location. Indicating different detonation techniques.

The committee machine produces 100% correct results with confidence measures that represent the probability of event-type occurrence within the holding cluster.

The current paper represents an idea to implement artificial intelligence to assist experts in decision-making situations. The committee machine could Identify the nature of a particular event using the aid of several discrimination methods. The proposed committee machine could combine the results of several algorithms and expert opinions to form one single output with a confidence measure.

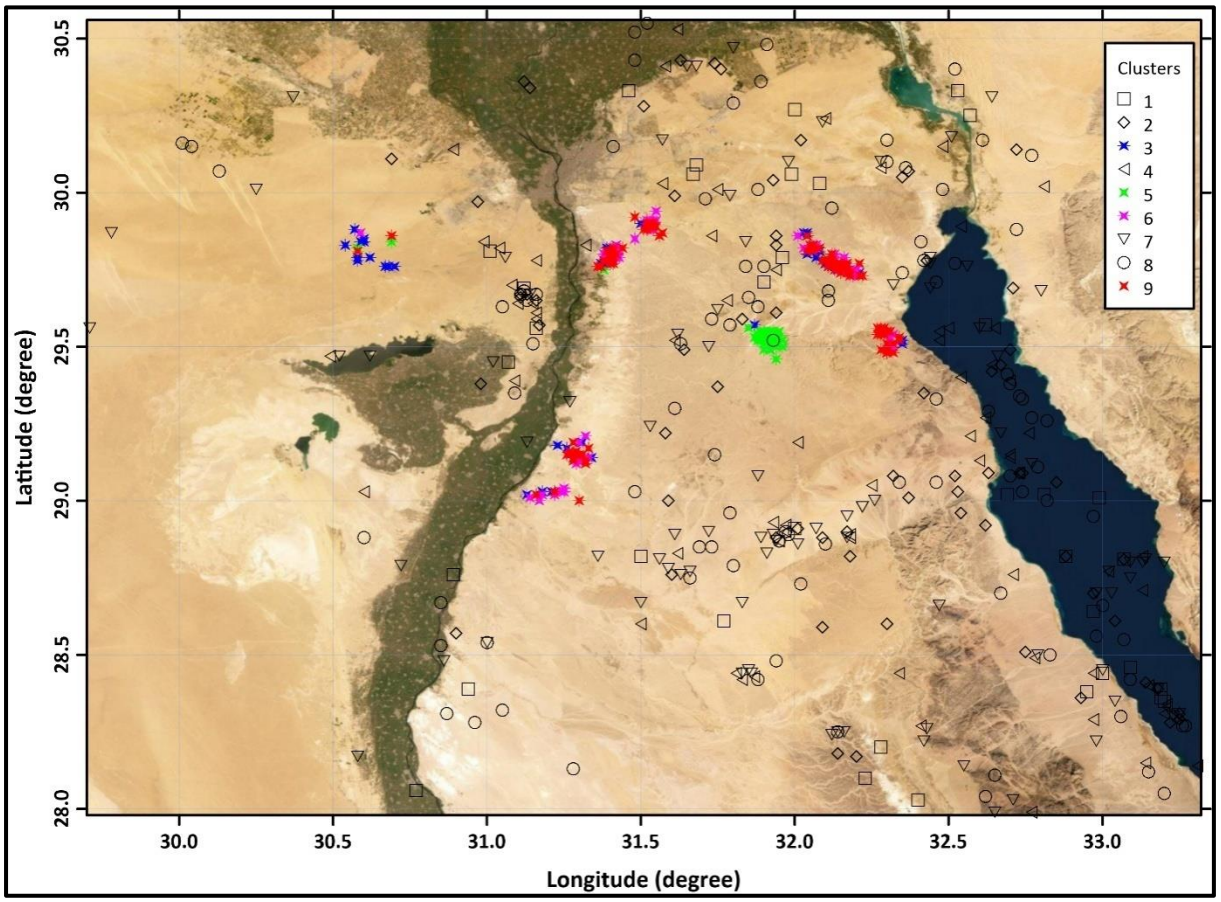

Figure 9: The spatial distribution of the 9 clusters SOM. The explosions are marked by asterisks and Earthquakes by other shapes. The green-colored asterisks (cluster 5) are almost concentrated in a single location. This indicates that this location has a special detonation characteristic.

Declarations

Funding

No funding was received for conducting this study.

Conflicts of interest/Competing interests

The authors have no conflicts of interest to declare that are relevant to the content of this article.

Authors' contributions

Ahmed Lethy performed the data analysis and wrote the manuscript; Adel S. Othman preparation of the data set; Mohamed N. ElGabry contributed to the conception of the study and revise the manuscript; Hesham Hussein revise the manuscript with constructive discussion; Gad El-Qady revise the manuscript.

Computer Code Availability

Source code of the proposed approach is available from the first author and can be download form https://github.com/Ahmedellethy/Discrimination
Name of Code: Machine Discriminator (MD)
Developer: Ahmed Lethy
Contact address *National Research Institute of Astronomy and Geophysics NRIAG, 1, El Marsad St. 11421, Helwan Egypt.*
E-mail alethy@nriag.sci.eg
Year first available 2021
Hardware: Intel or AMD x86-64 processor with four logical cores and AVX2 instruction set support with 4 GB ram
Program language: Matlab
Program size: about 33 kb

References

1. Bennett, T. J. & Murphy, J. R. Analysis of seismic discrimination capabilities using regional data from western United States events. *Bull. Seismol. Soc. Am.* **76**, 1069–1086 (1986).

2. Wuster, J. Discrimination of chemical explosions and earthquakes in central Europe - a case study. *Bull. - Seismol. Soc. Am.* **83**, (1993).

3. Plafcan, D. *et al.* Regional discrimination of chemical explosions and earthquakes: A case study in Morocco. *Bull. Seismol. Soc. Am.* **87**, (1997).

4. Mclaughlin, K. L., Bonner, J. L. & Barker, T. Seismic source mechanisms for quarry blasts: modelling observed Rayleigh and Love wave radiation patterns from a Texas quarry. *Geophys. J. Int* **156**, 79–93 (2004).

5. Allmann, B. P., Shearer, P. M. & Hauksson, E. Spectral discrimination between quarry blasts and earthquakes in southern California. *Bull. Seismol. Soc. Am.* **98**, 2073–2079 (2008).

6. Gitterman, Y., Pinsky, V. & Shapira, A. *Spectral classification methods in monitoring small local events by the Israel seismic network*. *Journal of Seismology* vol. 2 (1998).

7. Gitterman, Y. & Van Eck, T. Spectra of quarry blasts and microearthquakes recorded at local distances in Israel. *Bull. - Seismol. Soc. Am.* **83**, (1993).

8. Hedlin, M. A. H. A global test of a time-frequency small-event discriminant. *Bull. Seismol. Soc. Am.* **88**, (1998).

9. Kim, S. G., Park, Y. C. & Kim, W. Y. Discrimination of small earthquakes and artificial

explosions in the Korean Peninsula using Pg/Lg ratios. *Geophys. J. Int.* **134**, 267–276 (1998).

10. Smith, A. T. Discrimination of explosions from simultaneous mining blasts. *Bull. - Seismol. Soc. Am.* **83**, (1993).

11. Taylor, S. R., Sherman, N. W. & Denny, M. D. Spectral discrimination between NTS explosions and Western United States earthquakes at regional distances. *Bull. - Seismol. Soc. Am.* **78**, (1988).

12. Walter, W. R., Mayeda, K. M. & Patton, H. J. Phase and spectral ratio discrimination between NTS earthquakes and explosions, Part I: empirical observations. *Bull. - Seismol. Soc. Am.* **85**, (1995).

13. Carr, D. B. & Garbin, H. D. Discriminating ripple-fired explosions with high-frequency (>16Hz) data. *Bull. Seismol. Soc. Am.* **88**, (1998).

14. Su, F., Aki, K. & Biswas, N. N. Discriminating quarry blasts from earthquakes using coda waves. *Bull. - Seismol. Soc. Am.* **81**, (1991).

15. Hartse, H. E., Phillips, W. S., Fehler, M. C. & House, L. S. Single-station spectral discrimination using coda waves. *Bull. - Seismol. Soc. Am.* **85**, (1995).

16. Agnew, D. C. The use of time-of-day seismicity maps for earthquake/explosion discrimination by local networks, with an application to the seismicity of San Diego County. *Bull. Seism. Soc. Am.* **80**, 747-750. (1990).

17. Wiemer, S. & Baer, M. Mapping and removing quarry blast events from seismicity catalogs. *Bull. Seismol. Soc. Am.* **90**, 525–530 (2000).

18. Orlic, N. & Loncaric, S. Earthquake—explosion discrimination using genetic algorithm-based boosting approach. *Comput. Geosci.* **36**, 179–185 (2010).

19. Kortström, J., Uski, M. & Tiira, T. Automatic classification of seismic events within a regional seismograph network. *Comput. Geosci.* **87**, 22–30 (2016).

20. Dowla, F. U., Taylor, S. R. & Anderson, R. W. Seismic discrimination with artificial neural networks: preliminary results with regional spectral data. *Bull. - Seismol. Soc. Am.* **80**, 1346–1373 (1990).

21. Mostafa Allameh Zadeh & Mohsen Farrokhi. Discrimination between Earthquakes and Explosions Using Artifi cial Neural Networks. *Am. J. Biometrics Biostat.* **2**, 1–6 (2018).

22. Benbrahim, M., Daoudi, A., Benjelloun, K. & Ibenbrahim, A. Discrimination of Seismic Signals Using Artificial Neural Networks. *World Acad. Sci. Eng. Technol.* **4**, 4–7 (2005).

23. Disha, S. A Study to Discriminate Earthquake from Mining Blast Using Neural Network. *Int. J. Res. Sci. Innov.* **III**, 106–108 (2015).

24. Mostafa AllamehZadeh. Discrimination between Earthquakes and Explosion Using MLP and RBF Neural Networks. *Biostat. Biometrics Open Access J.* **2**, 1–13 (2017).

25. Yıldırım, E., Gülbağ, A., Horasan, G. & Doğan, E. Discrimination of quarry blasts and earthquakes in the vicinity of Istanbul using soft computing techniques. *Comput. Geosci.* **37**, 1209–1217 (2011).

26. Tiira, T. Discrimination of nuclear explosions and earthquakes from teleseismic distances with

a local network of short period seismic stations using artificial neural networks. *Phys. Earth Planet. Inter.* **97**, 247–268 (1996).

27. Del Pezzo, E. *et al.* Discrimination of earthquakes and underwater explosions using neural networks. *Bull. Seismol. Soc. Am.* **93**, 215–223 (2003).

28. AbdelHafiez, H. E. & Tawfiek, A. A review of the Egyptian National Seismological Network after 20 years of operation. *NRIAG J. Astron. Geophys.* **9**, (2020).

29. Abdel Hafiez, H. E. & Toni, M. Ambient Noise Level and Site Characterization in Northern Egypt. *Pure Appl. Geophys.* **176**, 2349–2366 (2019).

30. NRIAG. *Egyptian Earthquake Bulletin (2019)*. (2020).

31. Kumar, A., Kumar, A., Mittal, H., Kumar, A. & Bhardwaj, R. Software to Estimate Earthquake Spectral and Source Parameters. *Int. J. Geosci.* **03**, 1142–1149 (2012).

32. Badawy, A. Discrimination of microearthquakes and quarry blasts: A case study in Northern Egypt. *Acta Geophys. Pol.* (2001).

33. Arrowsmith, S. J., Hedlin, M. A. H., Arrowsmith, M. D. & Stump, B. W. Identification of delay-fired mining explosions using seismic arrays: Application to the PDAR Array in Wyoming, USA. *Bull. Seismol. Soc. Am.* (2007) doi:10.1785/0120060136.

34. Baumgardt, D. R. & Ziegler, K. A. Spectral evidence for source multiplicity in explosions: application to regional discrimination of earthquakes and explosions. *Bull. - Seismol. Soc. Am.* (1988).

35. Hedlin, M. A. H., Minster, J. B. & Orcutt, J. A. The time—frequency characteristics of quarry blasts and calibration explosions recorded in Kazakhstan, USSR. *Geophys. J. Int.* **99**, 109–122 (1989).

36. Kim, W. Y., Simpson, D. W. & Richards, P. G. High-frequency spectra of regional phases from earthquakes and chemical explosions. *Bull. - Seismol. Soc. Am.* (1994) doi:10.1016/0148-9062(95)93187-t.

37. Kiszely, M. Discrimination of quarry-blasts from earthquakes using spectral analysis and coda waves in Hungary. *Acta Geod. Geophys. Hungarica* (2001) doi:10.1556/AGeod.36.2001.4.5.

38. Stump, B. W., Hedlin, M. A. H., Pearson, D. C. & Hsu, V. Characterization of mining explosions at regional distances: Implications with the international monitoring system. *Rev. Geophys.* (2002) doi:10.1029/1998RG000048.

39. Tiira, T. Detecting teleseismic events using artificial neural networks. *Comput. Geosci.* **25**, 929–938 (1999).

40. Moya, A. & Irikura, K. Inversion of a velocity model using artificial neural networks. *Comput. Geosci.* **36**, 1474–1483 (2010).

41. Haykin, S. S. *Neural Networks: A Comprehensive Foundation 2Nd Ed.* (Prentice-Hall Of India Pvt. Limited, 1999).

42. Mehrotra, K., Mohan, C. & Ranka, S. *Elements of Artificial Neural Networks*. (The MIT Press, 1996). doi:10.7551/mitpress/2687.001.0001.

43. Abiodun, O. I. *et al.* State-of-the-art in artificial neural network applications: A survey. *Heliyon*

(2018) doi:10.1016/j.heliyon.2018.e00938.

44. Levenberg, K. A method for the solution of certain non-linear problems in least squares. *Q. Appl. Math.* (1944) doi:10.1090/qam/10666.

45. Marquardt, D. W. An Algorithm for Least-Squares Estimation of Nonlinear Parameters. *J. Soc. Ind. Appl. Math.* **11**, (1963).

46. CÖMERT, Z. & KOCAMAZ, A. A Study of Artificial Neural Network Training Algorithms for Classification of Cardiotocography Signals. *Bitlis Eren Univ. J. Sci. Technol.* **7**, 93–103 (2017).

47. Singh, A., Saxena, P. & Lalwani, S. A Study of Various Training Algorithms on Neural Network for Angle based Triangular Problem. *Int. J. Comput. Appl.* **71**, 30–36 (2013).

48. Urolagin, S., K.V., P. & Reddy, N. V. S. Generalization Capability of Artificial Neural Network Incorporated with Pruning Method. in *Advanced Computing, Networking and Security* (eds. Thilagam, P. S., Pais, A. R., Chandrasekaran, K. & Balakrishnan, N.) 171–178 (Springer Berlin Heidelberg, 2012).

49. Agrawal, R., Imieliński, T. & Swami, A. Mining Association Rules Between Sets of Items in Large Databases. *ACM SIGMOD Rec.* **22**, 207–216 (1993).

50. Lai, K. & Cerpa, N. Support vs Confidence in Association Rule Algorithms. in *OPTIMA* (2001).

51. Du, K. L. Clustering: A neural network approach. *Neural Networks* **23**, 89–107 (2010).

52. Flexer, A. On the use of self-organizing maps for clustering and visualization. *Lect. Notes Comput. Sci. (including Subser. Lect. Notes Artif. Intell. Lect. Notes Bioinformatics)* **1704**, 80–88 (1999).

53. Roden, R., Smith, T. A., Santogrossi, P., Sacrey, D. & Jones, G. Seismic interpretation below tuning with multiattribute analysis. *Lead. Edge* **36**, 330–339 (2017).

54. Köhler, A., Ohrnberger, M. & Scherbaum, F. Unsupervised pattern recognition in continuous seismic wavefield records using Self-Organizing Maps. *Geophys. J. Int.* **182**, 1619–1630 (2010).

55. Kuyuk, H. S., Yildirim, E., Dogan, E. & Horasan, G. An unsupervised learning algorithm: Application to the discrimination of seismic events and quarry blasts in the vicinity of Istanbul. *Nat. Hazards Earth Syst. Sci.* **11**, 93–100 (2011).

56. Messina, A. & Langer, H. Pattern recognition of volcanic tremor data on Mt. Etna (Italy) with KKAnalysis—A software program for unsupervised classification. *Comput. Geosci.* **37**, 953–961 (2011).

57. Arsuaga, U. E. & Martín, D. F. Topology Preservation in SOM. *World Acad. Sci. Eng. Technol.* **21**, 991–994 (2008).

58. Panda, S. S. Self Organizing Map (SOM) Usage in LULC Classification. in *Encyclopedia of GIS* (eds. Shekhar, S. & Xiong, H.) 1036–1042 (Springer US, 2008). doi:10.1007/978-0-387-35973-1_1181.

59. López-Rubio, E. & DíazRamos, A. Grid topologies for the self-organizing map. *Neural Networks* **56**, 35–48 (2014).

60. Cabanes, G. & Bennani, Y. Learning topological constraints in self-organizing map. *Lect. Notes Comput. Sci. (including Subser. Lect. Notes Artif. Intell. Lect. Notes Bioinformatics)* **6444 LNCS**,

367–374 (2010).

61. Hartigan, J. A. *Clustering Algorithms*. (John Wiley & Sons, Inc., 1975).

62. Hartigan, J. A. & Wong, M. A. Algorithm AS 136: A K-Means Clustering Algorithm. *Appl. Stat.* (1979) doi:10.2307/2346830.

63. Boehmke, B., Greenwell, B., Boehmke, B. & Greenwell, B. K-means Clustering. in *Hands-On Machine Learning with R* (2020). doi:10.1201/9780367816377-20.

64. MacQueen, J. Some methods for classification and analysis of multivariate observations. in *Proceedings of the Fifth Berkeley Symposium on Mathematical Statistics and Probability, Volume 1: Statistics* 281–297 (University of California Press, 1967).

65. Kuyuk, H. S., Yildirim, E., Dogan, E. & Horasan, G. Application of k-means and Gaussian mixture model for classification of seismic activities in Istanbul. *Nonlinear Process. Geophys.* **19**, 411–419 (2012).

66. Bishop, C. M. *Machine Learning and Pattern Recogniton*. *Information Science and Statistics* (2006).

67. Carmichael, C. G. & Bartlett, E. B. Stacking diverse models to achieve reliable error response distributions. *Int. J. Smart Eng. Syst. Des.* **4**, 31–39 (2002).

68. Mazurov, V. D. & Polyakova, E. Y. Committees: History and Applications in Machine Learning. in *Mathematical Optimization Theory and Operations Research* (eds. Bykadorov, I., Strusevich, V. & Tchemisova, T.) 3–16 (Springer International Publishing, 2019).

69. Nadiri, A. A., Fijani, E., Tsai, F. T. C. & Moghaddam, A. A. Supervised committee machine with artificial intelligence for prediction of fluoride concentration. *J. Hydroinformatics* **15**, 1474–1490 (2013).

70. Pandey, T. N., Jagadev, A. K., Dehuri, S. & Cho, S. B. A novel committee machine and reviews of neural network and statistical models for currency exchange rate prediction: An experimental analysis. *J. King Saud Univ. - Comput. Inf. Sci.* (2018) doi:10.1016/j.jksuci.2018.02.010.